

Metal-semiconductor-metal neutron detectors based on hexagonal boron nitride epitaxial layers

S. Majety, J. Li, X. K. Cao, R. Dahal, J. Y. Lin and H. X. Jiang^{a)}

Dept. of Electrical and Computer Engineering, Texas Tech University, Lubbock, TX 79409

ABSTRACT

Hexagonal boron nitride (hBN) possesses extraordinary potential for solid-state neutron detector applications. This stems from the fact that the boron-10 (^{10}B) isotope has a capture cross-section of 3840 barns for thermal neutrons that is orders of magnitude larger than other isotopes. Epitaxial layers of hBN have been synthesized by metal organic chemical vapor deposition (MOCVD). Experimental measurements indicated that the thermal neutron absorption coefficient and length of natural hBN epilayers are about $0.0036\ \mu\text{m}^{-1}$ and $277\ \mu\text{m}$, respectively. To partially address the key requirement of long carrier lifetime and diffusion length for a solid-state neutron detector, micro-strip metal–semiconductor–metal detectors were fabricated and tested. A good current response was generated in these detectors using continuous irradiation with a thermal neutron beam, corresponding to an effective conversion efficiency approaching ~80% for absorbed neutrons.

Keywords: Semiconducting hexagonal boron nitride, solid-state neutron detectors, MOCVD growth, epitaxial layers

1. INTRODUCTION

Neutron detectors with improved detection efficiency are highly sought after for a range of applications including fissile materials sensing, neutron therapy, medical imaging, the study of materials sciences, probing of protein structures, and oil exploration and would provide critical technologies which can support counter-proliferation and counter-terrorism missions¹. Due to the high performance, ^3He gas-filled devices have been widely deployed. The major advantage of ^3He gas-filled devices is their intrinsically low background count (and hence high detection efficiency). However, the most serious issue is that there is a significant shortage of ^3He gas². Thus, there is an urgent need to develop advanced materials to enable high efficiency solid-state neutron detectors.

Thermal neutrons (0.025 eV) have a low probability of interacting with conventional semiconductor materials. Thus, a two step detection process is generally required for a solid-state detector³⁻⁹. First, the thermal neutrons are converted to energetic ions by a material with a high thermal neutron capture cross-section. The element boron (B) has been the material of choice because of its very high thermal neutron cross-section. Second, the energetic ions are then collected using a semiconductor detector.

The element boron exists as two main isotopes, boron-10 (^{10}B) and boron-11 (^{11}B) in a natural abundance of approximately 20% and 80%, respectively¹¹. The ^{10}B isotope is particularly useful for neutron detection because its thermal (energy of 0.025 eV) neutron capture cross-section is several orders of magnitude larger than that of most isotopes (3850 barns)^{10,11}. When a ^{10}B atom captures a neutron, it undergoes the following nuclear reaction:



Solid-state neutron detectors have recently been under rapid development³⁻⁹. The dominant approach employs the aforementioned two step process by coating a layer of boron containing neutron-to-alpha particle converter material onto a semiconductor such as Si or GaAs³⁻⁹. The as-created alpha particles in the boron material

travel to the semiconductor and lose their energy by producing a cloud of electron-hole pairs in Si, which serve as the detection signal for neutrons. The efficiency of such conversion devices is inherently low (2-5%) since the two functions (neutron capture and electrical signal generation) occur in separate layers and there are conflicting thickness requirements of the converter layer. The boron (or boron containing) layer must be thick enough to capture the incoming neutron flux, yet sufficiently thin to allow α particles to penetrate into the semiconductor layer to generate electron and hole (e-h) pairs. The typical mean free path of α particles in B is $\sim 3.3 \mu\text{m}^4$. Reducing the boron layer thickness reduces the distance the α particles must travel, but at a cost of reduced neutron absorption. Detection efficiency can be improved by preparing closely spaced alternating pillar arrays (3-D pillar and trench structures) of boron and semiconductor.⁶⁻⁹ However, an extremely high aspect ratio (a 100 nm pitch and 50 μm etch depth of pillars) is required to obtain a maximum theoretical efficiency of $\sim 85\%$ ^{2,4,7-9} a rather challenging task to be realized experimentally.

The efficiency of solid-state neutron detectors can be greatly improved by combining the neutron capture and charge collection layers together in a *single* semiconducting material. This can be achieved by fabricating the device with a boron based semiconductor. With neutron capture, charge collection, and electrical signal generation occurring in a single semiconductor material, the signal loss that is inherent in current existing solid-state detectors can be eliminated. In principle, if synthesized using an isotopically-enriched boron-10 (^{10}B) precursor, the neutron detection efficiency of boron based devices can approach 100%. Boron based neutron detectors in principle will be semiconductor detectors, which neutrally possess all the wonderful advantages resulting from the 50-year R & D of semiconductor technologies.

There have been many efforts to make neutron detectors from boron-based semiconductors¹²⁻¹⁹. Examples include the use of alpha-rhombohedral boron¹², thin ($< 2 \mu\text{m}$) polycrystalline or amorphous boron carbide (B_4C)¹⁵⁻¹⁸, pyrolytic boron nitride (BN)^{14,19}, and composite BN²⁰. However, the full potential of semiconductor technologies has not been realized due to the material's porosity and disordered polycrystalline or amorphous nature and inability of conductivity control. Here, we report the growth and characterization of semiconducting hexagonal BN (hBN) epilayers and the demonstration of a micro-strip planar metal-semiconductor-metal (MSM) detector.

2. EXPERIMENT

Hexagonal BN epitaxial layers of about 1 μm in thickness were synthesized by metal organic chemical vapor deposition (MOCVD) using natural triethylboron (TEB) sources (containing 19.8% of ^{10}B and 80.2% of ^{11}B) and ammonia (NH_3) as B and N precursors, respectively. Prior to epilayer growth, a 20 nm BN or AlN buffer layer was first deposited on sapphire substrate at 800 $^\circ\text{C}$. The typical hBN epilayer growth temperature was about 1300 $^\circ\text{C}$. X-ray diffraction (XRD) was employed to determine the lattice constant and crystalline quality of the epilayers^{21,22}. XRD θ -2 θ scan revealed a *c*-lattice constant $\sim 6.67 \text{ \AA}$, which closely matches the bulk *c*-lattice constant of hBN ($c=6.66 \text{ \AA}$)²³⁻²⁵, affirming that BN films are of a single hexagonal phase. Figure 1(a) shows the XRD measurement results performed on a 1 μm thick hBN film. The rocking curve of the (002) reflection possesses a full width at half maximum (~ 385 arcsec), which is a dramatic improvement over previously reported values for hBN films (1.5^0 - 0.7^0)²⁶, but is comparable to that of a typical GaN epilayer grown on sapphire with a similar layer thickness²⁷, revealing a relatively high crystalline quality of the MOCVD grown hBN epilayers. The results of secondary ion mass spectrometry (SIMS) measurements (performed by EAG Lab - Evans Analytical Group) shown in Fig. 1(b) revealed that hBN epilayers have excellent stoichiometry. Room temperature (300 K) and low temperature (10 K) PL spectra for hBN grown on sapphire substrates are shown in Fig. 2 (top and bottom respectively). PL spectra measured at 10K shows a dominant band-edge related emission at ~ 5.48 eV.

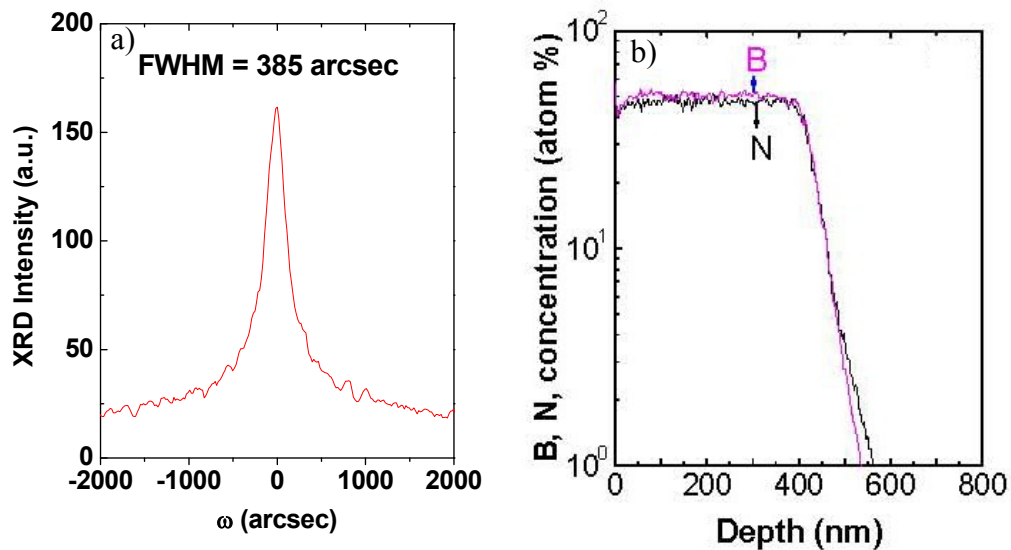


Fig. 1(a) X-ray diffraction rocking curve of the (002) reflection of an hBN epilayer grown on sapphire substrate. (b) SIMS measurement results performed on this epilayer²².

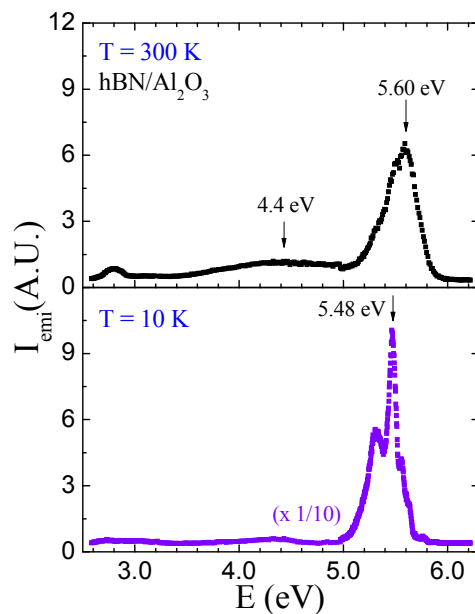


Fig. 2 Representative photoluminescence (PL) spectra of our hBN epilayers measured at 300 K (top) and 10 K (bottom).

The high electrical resistivity of $\sim 10^{13} \Omega\text{-cm}$ in undoped hBN epilayers make them suitable for the fabrication of MSM detectors with extremely low dark current. To partially address the key requirement of long carrier lifetime and diffusion length for a solid-state neutron detector, metal–semiconductor–metal detectors with micro-strip geometry instead of a pure planar geometry were fabricated. Figure 3(a) depicts a packaged hBN micro-strip MSM neutron detector (bonded device). The fabrication procedures consisted of the following steps. First, photolithography was employed to define the micro-scale strips (5 $\mu\text{m}/5 \mu\text{m}$ width/spacing), followed by pattern transferring using inductively-coupled plasma dry etching to form micro-strips. A bilayer of 5 nm/5 nm (Ni/Au) was deposited using e-beam evaporation to form the Schottky contacts. Bonding pads were then formed by depositing

an Au (200 nm) layer. Figure 3 (b) shows the fabricated detector. The sapphire substrate was then polished and thinned to about 100 μm and diced to discrete devices, which were bonded onto device holders for characterization. Preliminary measurements of interactions between neutrons and hBN materials were carried out at the Kansas State University TRIGA Mark II Reactor. The thermal neutron (0.025 eV) flux was set to about $6.2 \times 10^4 / \text{cm}^2 \cdot \text{s}$ for the experiment. The system for the steady current response measurements consisted of a source-meter and an electrometer connected in series.

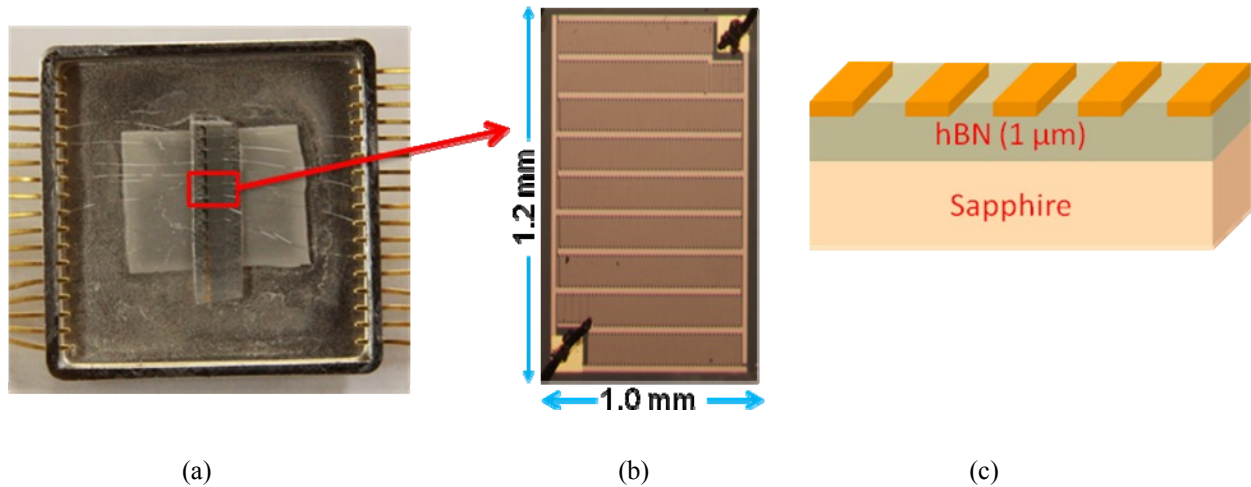


Fig. 3 (a) Micrograph showing a packaged hBN micro-strip MSM neutron detector indicating (b) a fabricated hBN micro-strip MSM neutron detector; (c) Schematic of the hBN MSM detector²¹.

3. RESULTS AND DISCUSSION

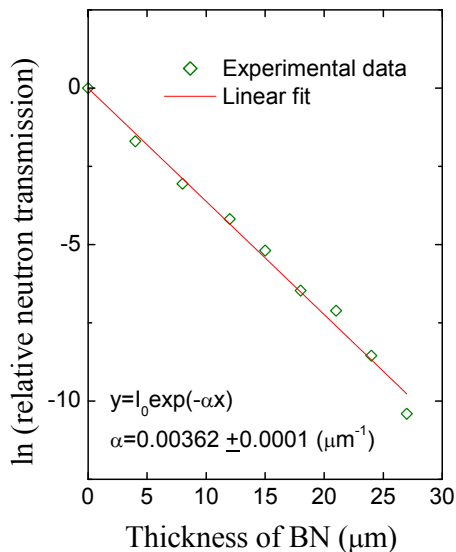


Fig. 4 Measured relative thermal neutron transmission in natural hBN epilayers²¹

Figure 4 shows the measured attenuation of normally incident thermal neutrons in hBN. In conducting the measurements, the variation in hBN epilayer thickness was accomplished by adding the number of hBN wafers in the thermal neutron beam path. The relative neutron transmission (T) is measured as a function of the thickness of hBN layers. As can be seen from Fig. 4, $\ln(T)$ decreases as the thickness of hBN layers increase. $\ln(T)$ is fitted linearly as a function of thickness in order to calculate the absorption coefficient (α) and absorption length (λ) of

$$\alpha = 0.0036 \mu\text{m}^{-1};$$

$$\lambda (=1/\alpha) = 277 \mu\text{m}$$

The microscopic thermal neutron absorption length can also be estimated by knowing the thermal neutron capture cross-section σ and density of ^{10}B in a hexagonal lattice of BN. We have

$$\sigma = 3.84 \times 10^3 \text{ barn} = 3.84 \times 10^3 \times 10^{-24} \text{ cm}^2 = 3.84 \times 10^{-21} \text{ cm}^2;$$

A hexagonal lattice of BN have lattice constants of $a=2.50 \text{ \AA}$ and $c=6.66 \text{ \AA}$, which yields, respectively, the density for natural boron $N_{[\text{B}]}$ and ^{10}B isotope $N_{[\text{B-10}]}$ as

$$N_{[\text{B}]} = 5.5 \times 10^{22} \text{ cm}^{-3},$$

$$N_{[\text{B-10}]} = 20\%N_{[\text{B}]} = 1.1 \times 10^{22} \text{ cm}^{-3}.$$

These together yield a theoretical microscopic neutron absorption coefficient (Σ) and absorption length (λ) in a natural hBN as

$$\Sigma = \sigma N_{[\text{B-10}]} = 3.84 \times 10^{-21} \text{ cm}^2 \times 1.1 \times 10^{22} \text{ cm}^{-3} = 42 \text{ cm}^{-1} = 4.2 \times 10^{-3} \mu\text{m}^{-1};$$

$$\lambda = 1/\Sigma = 238 \mu\text{m}.$$

Thus, the estimated microscopic neutron absorption length is in close agreement with the measured value of 277 μm .

The absolute current response of the detector to a continuous irradiation of thermal neutron beam was measured. Although the neutron absorption layer in our devices was only 1 μm , signal generation was evident. This is attributed to the unique micro-strip device architecture shown schematically in Fig. 3(c) which not only effectively utilizes the outstanding lateral transport properties of hBN, but also alleviates, to a certain degree, the stringent requirement of the large carrier diffusion length needed to ensure a maximum sweep out of electrons and holes at metal contacts. As illustrated in Fig. 5, it was found that the detectors have low background current and continuous irradiation by the thermal neutron beam at a flux of $6.2 \times 10^4 / \text{cm}^2 \cdot \text{s}$ generates a steady current response of about 0.085 pA, independent of the applied voltage in the measured range (20 to 100 V).

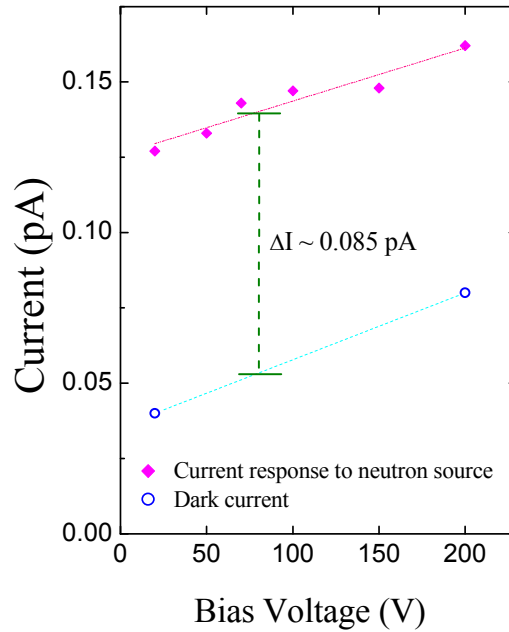


Fig. 5 Steady current response in the hBN micro-strip MSM detector (1 mm x 1.2 mm) fabricated from an epilayer of 1 μm in thickness, subjected to a continuous irradiation with thermal neutron (0.025 eV) beam at a flux of $6.2 \times 10^4 / \text{cm}^2 \cdot \text{s}^{21}$.

We can also estimate the carrier generation rate and magnitude of electrical current signal generated by the continuous irradiation of a thermal neutron beam by considering the dominant nuclear reaction described by Eq. (2). Based on the neutron beam flux (N_{flux}) used for the experiment, the measured neutron absorption length (λ), and device layer thickness ($t=1 \mu\text{m} \ll \lambda$), the effective absorbed neutron flux (N^*_{flux}) by the detector can be calculated and is

$$N^*_{\text{flux}} = (t/\lambda) N_{\text{flux}} = (1\mu\text{m}/277 \mu\text{m}) \times 6.2 \times 10^4 / \text{cm}^2 \cdot \text{s} = 2.2 \times 10^2 / \text{cm}^2 \cdot \text{s}.$$

On the other hand, the energy required to generate one electron-hole (e^-h^+) pair is about three times of the bandgap energy ($\sim 18 \text{ eV}$ in hBN)¹⁰. Based on the dominant nuclear reaction described by Eq. (2), each absorbed neutron is expected to generate daughter particles (Li and α) with kinetic energies of 2.310 MeV (94%) and 2.792 MeV (6%), giving an average energy of 2.34 MeV, or equivalently $1.3 \times 10^5 e^-h^+$ pairs ($=2.34 \text{ MeV}/18 \text{ eV}$). Therefore, the free electron generation rate (n) would be $n=N^*_{\text{flux}} \times 1.3 \times 10^5$, or

$$n = 2.2 \times 10^2 / \text{cm}^2 \cdot \text{s} \times 1.3 \times 10^5 = 2.9 \times 10^7 / \text{cm}^2 \cdot \text{s}.$$

The magnitude of response current (I) can be estimated by knowing the device area ($A=1.2 \text{ mm}^2=1.2 \times 10^{-2} \text{ cm}^2$) as

$$I = 2 \times 2.9 \times 10^7 / \text{cm}^2 \cdot \text{s} \times 1.2 \times 10^{-2} \text{ cm}^2 (e) = 7.0 \times 10^5 \times 1.6 \times 10^{-19} (\text{A}) \sim 1.1 \times 10^{-13} (\text{A}),$$

where the factor of 2 accounts for both the electron and hole conduction. Thus, the expected current of 0.11 pA is in accordance with the experimentally measured result of 0.085 pA. This close agreement between the expected and measured response currents not only provides high confidence in the measurement results, but also implies that the measured performance of the detector is at 77% ($=0.085/0.11$) of the theoretically predicted.

4. SUMMARY

We believe that hBN based semiconductor neutron detectors have the potential to revolutionize neutron detection. With BN neutron capture, charge collection, and electrical signal generation occurring in a single material, the signal loss that is inherent in current existing solid-state detectors can be eliminated. With further developments in material growth, doping control^{22,28} and device design such as incorporating thick ¹⁰B enriched epilayers (or multiple ¹⁰B enriched epilayers) with improved crystalline quality and more sophisticated device structures such as p-i-n junctions, and novel device architectures to effectively utilize the excellent lateral transport properties of hBN, in principle, the neutron detection efficiency of hBN semiconductor detectors can be very high. Furthermore, the ability of producing wafer scale hBN semiconducting materials by techniques such as MOCVD also opens the possibility to construct relative large area detectors as well as two-dimensional array neutron cameras.

ACKNOWLEDGEMENTS

The neutron detector work is support by DHS/NSF ARI Program (CBET-1038700 managed by Dr. Mark Wrobel). Epitaxial growth of hBN work is also supported in part by DRAPA-CMUVT (managed by Dr. John Albrecht). The authors are grateful to Dr. Jeffrey Geuther for his help with the neutron detection experiment and coordination with the Kansas State University TRIGA Mark II Reactor facility. Jiang and Lin are grateful to the AT&T Foundation for the support of Ed Whitacre and Linda Whitacre Endowed chairs.

REFERENCES:

a) hx.jiang@ttu.edu

- [1] Spowart, A. R., "Design of Neutron Detectors Utilising Luminescent Glass," IEEE Trans. Nucl. Sci., 31(1), 269-273 (1984).
- [2] Kouzes, R. L., "The ^3He Supply Problem, April 2009; Pacific Northwest National Laboratory;" Prepared for the U.S. Department of Energy under Contract DE-AC05-76RL01830, http://www.pnl.gov/main/publications/external/technical_reports/PNNL-18388.pdf.
- [3] Rose, A., "Sputtered boron films on silicon surface barrier detectors," Nucl. Inst. Meth. Res. A, 52(1), 166 (1967).
- [4] Nikolic, R. J., Cheung, C. L., Reinhardt, C. E., Wang, T. F., "Future of semiconductor based thermal neutron detectors," UCRL-PROC-219274, Nanotech 2006, Boston (2006).
- [5] Gersch, H. K., McGregor, D. S., and Simpson, P. A., "The effect of incremental gamma-ray doses and incremental fluences upon the performance of self-biased ^{10}B -coated high-purity epitaxial GaAs thermal neutron detectors," Nucl. Inst. Meth. Phys. Res. A, 489(1-3), 85-98 (2002).
- [6] LiCausi, N., Dingley, J., Danon, Y., Lu, J.-Q., and Bhat, I. B., "A novel solid-state self powered neutron detector," Proc. SPIE 7079, 707908 (2008).
- [7] Nikolic, R. J., Conway, A. M., Reinhardt, C. E., Graff, R., Wang, T. F., Deo, N., and Cheung, C. L., "6:1 aspect ratio silicon pillar based thermal neutron detector filled with ^{10}B ," Appl. Phys. Lett., 93(13), 133502 (2008).
- [8] Nikolic, R. J., Cheung, C. L., Reinhardt, C. E., and Wang, T. F., "Roadmap for High Efficiency Solid-State Neutron Detectors," Proc. SPIE 6013, 601305 (2005).
- [9] Conway, A. M., Wang, T. F., Deo, N., Cheung, C. L., and Nikolic, R. J., "Numerical simulations of pillar structured solid state thermal neutron detector: efficiency and gamma discrimination," IEEE Trans. Nucl. Sci., 56(5), 2802-2807 (2009)
- [10] Knoll, G. F., [Radiation detection and measurement], 4th edition, John Wiley & Sons, (2010).
- [11] Osberghaus, O., "Isotopic abundance of boron. Mass-spectrometric investigation of the electron-impact products of boron trifluoride and boron trichloride," Zeitschrift fuer Physik, 128(3), 366 (1950).
- [12] Wald, F., and Bullitt, J., "Semiconductor neutron detectors," U. S. Nat. Tech. Inform. Serv., AD-771526/1 (1973).
- [13] Ananthanarayanan, K. P., Gielisse, P. J. and Choudry, A., "Boron compounds for thermal-neutron detection," Nucl. Inst. Meth., 118(1), 45-48 (1974).
- [14] McGregor, D. S., Unruh, T. C., and McNeil, W.J., "Thermal neutron detection with pyrolytic boron nitride," Nucl. Instr. Meth. Phys. Res. A, 591(3), 530 (2008).
- [15] Lunca-Popa, P., Brand, J. I., Balaz, S., Rosa, L.G., Boag, N. M., Bai, M. , Robertson, B. W. and Dowben, P. A., "Evidence for multiple polytypes of semiconducting boron carbide (C_2B_{10}) from electronic structure," J. Phys. D. Appl. Phys., 38(8), 1248-1252 (2005).
- [16] Adenwalla, S., Welsch, P., Harken, A., Brand, J. I., Sezer, A. and Robertson, B. W., "Boron/n-silicon carbide heterojunction diodes," Appl. Phys. Lett., 79(26), 4357 (2001).
- [17] Harken, A. D., Day, E. E., Robertson, B. W., and Adenwalla, S., "Boron-rich semiconducting boron carbide neutron detector," Jpn. J. Appl. Phys. Pt. 1, 44, 444-445 (2005).
- [18] Osberg, K., Schemm, N., Balkir, S., Brand, J. O., Hallbeck, M. S., Dowben, P. A., and Hoffman, M. W., "A Handheld Neutron-Detection Sensor System Utilizing a New Class of Boron Carbide Diode," IEEE Sensor J., 6 (6), 1531-1538 (2006).
- [19] Doty, F. P., "Advanced digital detectors for neutron imagining," Sandia Report SAND2003-8796 (Sandia National Laboratories, Livermore, 2003).
- [20] Uher, J., Pospisil, S., Linhart, V., and Schieber, M., "Efficiency of composite boron nitride neutron detectors in comparison with helium-3 detectors," Appl. Phys. Lett., 90(12), 124101 (2007).
- [21] Li, J., Dahal, R., Majety, S., Lin, J. Y., and Jiang, H. X., "Hexagonal boron nitride epitaxial layers as neutron detector materials," Nucl. Instr. Meth. Phys. Res. A, 654(1), 417 (2011).
- [22] Dahal, R., Li, J., Majety, S., Pantha, B. N., Cao, X. K., Lin, J. Y., and Jiang, H. X., "Epitaxially grown semiconducting hexagonal boron nitride as a deep ultraviolet photonic material," Appl. Phys. Lett., 98(21), 211110 (2011).
- [23] Siklitsky, V., "Boron Nitride," <http://www.ioffe.rssi.ru/SVA/NSM/Semicond/BN/index.html>.

- [24] Rumyantsev, S. L., Levinshtein, M. E., Jackson, A. D., Mohammad, S. N., Harris, G. L., Spencer, M. G, Shur, M. S., [Properties of Advanced Semiconductor Materials GaN, AlN, InN, BN, SiC, SiGe .], John Wiley & Sons, Inc., New York, 67-92 (2001).
- [25] Lynch, R. W., and Drickamer, H. G. J., "Effect of High Pressure on the Lattice Parameters of Diamond, Graphite, and Hexagonal Boron Nitride," *J. Chem. Phys.* 44(1), 181 (1966).
- [26] Kobayashi, Y., Akasaka, T., and Makimoto, T., "Hexagonal boron nitride grown by MOVPE," *J. Crystal Growth*, 310(23), 5048-5052 (2008).
- [27] Nakamura, S., Fasol, G., and Pearton, S. J., *The blue laser diode: the complete story*, Springer, New York, (2000).
- [28] Majety, S., Li, J., Cao, X. K., Dahal, R., Pantha, B. N., Lin, J. Y., and Jiang, H. X., "Epitaxial growth and demonstration of hexagonal BN/AlGaIn p-n junctions for deep ultraviolet photonics," *Appl. Phys. Lett.*, 100(6), 061121 (2012).